

## Electrogeneration of hydrogen peroxide in acid medium using pyrolyzed cobalt-based catalysts: Influence of the cobalt content on the electrode performance

N. GUILLET<sup>1</sup>, L. ROUÉ<sup>1,\*</sup>, S. MARCOTTE<sup>1</sup>, D. VILLERS<sup>1</sup>, J.P. DODELET<sup>1</sup>, N. CHHIM<sup>2</sup> and S. TRÉVIN<sup>2</sup>  
<sup>1</sup>INRS – Énergie, Matériaux et Télécommunications, 1650 boul. Lionel Boulet, Varennes, Québec, J3X 1S2, Canada  
<sup>2</sup>Électricité de France – Centre de Recherche E.P.I./E23, Site des Renardières – Écuellen, 77818, Moret sur Loing, France

(\*author for correspondence, tel.: +1-450-9298185, fax: +1-450-9298198, e-mail: roue@emt.inrs.ca)

Received 31 October 2004; accepted in revised form 11 April 2005

**Key words:** cobalt, CoTMPP, electrocatalysis, gas diffusion electrode, H<sub>2</sub>O<sub>2</sub> production, oxygen reduction

### Abstract

Cobalt tetramethoxyphenyl porphyrin (CoTMPP) adsorbed on a high area carbon support (Vulcan XC72-R) and heat-treated at 900 °C under inert atmosphere was studied as electrocatalyst for the reduction of O<sub>2</sub> to H<sub>2</sub>O<sub>2</sub> in acid medium. Experiments performed on rotating ring-disc electrode (RRDE) and gas diffusion electrode (GDE) show that the catalyst performance depends on the cobalt loading, going through a maximum at 0.2 wt. % Co. For higher cobalt loadings, a growing part of oxygen is reduced into water, decreasing therefore the selectivity of the catalyst. These results are interpreted in terms of a further reduction of H<sub>2</sub>O<sub>2</sub> on Co-based catalytic sites before leaving the catalytic layer. For a GDE polarized at –150 mV vs. saturated calomel electrode (SCE) and loaded with 0.9 μg cm<sup>-2</sup> of 0.2 wt. % Co-based catalyst, a H<sub>2</sub>O<sub>2</sub> production rate of 300 μmol h<sup>-1</sup> cm<sup>-2</sup> was obtained which is five times higher than the H<sub>2</sub>O<sub>2</sub> production rate measured with Vulcan. In these conditions, the selectivity of the Co-based catalyst for H<sub>2</sub>O<sub>2</sub> production is 92%. The good agreement observed between RRDE and GDE results confirms the relevance of using RRDE experiment for screening these non-precious metal catalysts for further GDE applications.

### 1. Introduction

Hydrogen peroxide (H<sub>2</sub>O<sub>2</sub>) is currently one of the most essential chemicals for pulp bleaching, waste treatment and chemical production and it is a promising oxidant for green chemistry in the near future. Hydrogen peroxide is mainly produced by the anthraquinone process [1, 2]. Because such a process requires very large infrastructure investments, it is not really appropriate for small or localized generation of hydrogen peroxide. In that case, electrochemical methods based on the two-electron reduction of oxygen offer some important advantages over the anthraquinone method, including higher purity, greater safety and lower infrastructure investment and maintenance costs as well as fewer separation steps, unwanted by-products and environmental concerns.

H<sub>2</sub>O<sub>2</sub> is already produced electrochemically in an on-site process for pulp bleaching by the so-called Dow process which is based on the reduction of O<sub>2</sub> on a trickle bed cell over a graphite cathode in aqueous alkaline solution [3–5]. However, the energy cost of this electrochemical process is high and its efficiency is low due to the limited solubility of oxygen in the electrolyte.

Moreover, hydrogen peroxide solutions produced according to this process are alkaline, affecting therefore the long-term stability of H<sub>2</sub>O<sub>2</sub>. Furthermore, this process is not suitable for applications requiring either a neutral or an acid pH. Besides H<sub>2</sub>O<sub>2</sub> production on trickle bed, catalyzed gas diffusion electrode (GDE) have also been used as cathodes to produce hydrogen peroxide by the reduction of oxygen in both alkaline [6–9] and acidic media [10]. These electrodes are usually made of a carbon cloth covered with a layer composed of a catalyst mixed with carbon black and a low proportion of PTFE. PTFE acts as binder and confers hydrophobic properties to the layer. The aqueous solution is then in contact with the catalyst, while O<sub>2</sub> diffuses from the opposite face of the electrode through the catalyst layer and is reduced to hydrogen peroxide at the catalyst/solution interphase [11, 12]. To be a viable candidate as cathode electrocatalyst for industrial hydrogen peroxide production, the catalytic material must favor the two-electron oxygen reduction reaction (ORR) at high current densities and with a low overpotential, in addition to be of low cost and durable (typically, several years).

Carbon-supported transition metal N<sub>4</sub>-chelates like porphyrins, phthalocyanines, and related compounds

have been extensively investigated as possible catalysts for oxygen reduction. The main problem with these organometallic-based materials is their instability in acidic electrolytes. However, a heat treatment enhances the stability of these compounds adsorbed on carbon as shown by Wiesener with various  $N_4$ -chelate catalysts including Co porphyrin-based compounds [13]. It has been proposed that during the high temperature heat treatments ( $>500\text{ }^\circ\text{C}$ ), the adsorbed metal chelates lose their aromatic ring structure and the central part of the macrocycle becomes chemically bound to the carbon surface [14–16]. It is not even necessary to pyrolyze metal  $N_4$ -chelates on carbon to obtain catalytic activity for oxygen reduction. Catalytic materials are also obtained by pyrolyzing metal salts or complexes adsorbed on carbon in the presence of a nitrogen precursor. Several works revealed that only three components are needed to form such an active site for the oxygen reduction: a transition metal precursor (salt, metallic macromolecule or oxide), a nitrogen donor and a carbon support [14, 17–24]. The activity and the selectivity of the catalyst is largely dependent on the nature of the transition metal precursor, on the nature of the carbon support and on the pyrolysis parameters [25–27]. To date, the most promising results for oxygen reduction into hydrogen peroxide have been obtained with cobalt-based materials [25, 28, 29] while iron-based catalysts mainly reduce oxygen into water [28, 30].

From the numerous potential cobalt precursors, cobalt tetramethoxyphenylporphyrin (CoTMPP) was chosen in the present work for its high electrocatalytic activity [26]. In this work, the influence of the cobalt loading on the electrocatalytic activity and selectivity of pyrolyzed Co-based materials for  $\text{H}_2\text{O}_2$  production will be studied by rotating ring-disc electrode (RRDE) and by GDE experiments. The relevance of using RRDE experiments for screening our electrocatalysts for further GDE applications will be established.

## 2. Experimental

### 2.1. Catalyst preparation

The carbon support used throughout this work was Vulcan XC-72 R from Cabot. It is a high surface area carbon black ( $250\text{ m}^2\text{ g}^{-1}$ ) with very low iron content (0.002 wt. %) [14, 27]. The first step of the catalyst preparation was the pyrolysis of the carbon support under an inert gas. The carbon powder was put in a quartz boat which was inserted in a 5 cm diameter quartz tube. The carbon support was heat-treated under argon atmosphere (oxygen  $<5$  ppm, moisture  $<4$  ppm) at  $900\text{ }^\circ\text{C}$  for 2 h and cooled to room temperature under the same argon flow.

Cobalt porphyrin (5,10,15,20 tetrakis(4-methoxyphenyl)21H,23H-cobalt<sup>II</sup> porphyrin), noted CoTMPP, was obtained from Aldrich. CoTMPP quantities needed to

prepare various cobalt loadings ranging between 0.1 and 2 wt. % Co were dissolved in a small amount of acetone (50 ml) and added to 1 g of heat-treated carbon support. The suspension was left under magnetic stirring for 2 h at room temperature. Next, the solvent was first evaporated on a heating plate. Before completion of solvent evaporation, the material was put in an oven at  $70\text{ }^\circ\text{C}$  where the powder was left to dry overnight. This powder (cobalt macrocycles adsorbed onto pretreated carbon support) was pyrolyzed at  $900\text{ }^\circ\text{C}$  for 2 h under argon. All Co loadings reported in this work refer to the metal Co amount in weight % with respect to Vulcan mass before its last heat-treatment leading to the catalyst.

A catalytic suspension was prepared by adding 10 mg of the catalyst powder to  $98\text{ }\mu\text{l}$  of a 5% Nafion in alcohol–water solution (from Aldrich) and  $350\text{ }\mu\text{l}$  of an ethanol–water mixture (20:80 vol.%). Nafion acts as an organic binder and is thought to enhance kinetics of oxygen reduction [31, 32]. The mixture was stirred for 30 min in an ultrasonic bath for homogenization.

### 2.2. Electrochemical measurements

#### 2.2.1. Rotating ring-disc electrode

These experiments were performed on a Pine Instrument system. The RRDE was a glassy carbon disk ( $0.1642\text{ cm}^2$ ) surrounded with a platinum ring (0.45 mm wide) and separated from the disk by an insulating Teflon ring (0.36 mm wide). The rotation rate was set to 200 rpm. The ring collection efficiency was  $N = 0.2$  (determined from the  $\text{Fe}^{\text{II}}/\text{Fe}^{\text{III}}$  redox system using a solution of  $\text{K}_3\text{Fe}(\text{CN})_6$ ).

Before catalyst deposition, the working ring-disk electrode was mechanically polished with  $0.1\text{ }\mu\text{m}$  diamond paste on a Nylon film. Then it was rinsed with de-ionized water, ultrasonically cleaned with methanol (1 min) and dried. A small amount ( $5\text{ }\mu\text{l}$ ) of the catalyst suspension was pipetted and carefully deposited to cover the glassy carbon disk surface. The solvent evaporated within a few minutes and the electrode holding the fine catalyst film was then ready for experiments.

RRDE experiments were conducted at room temperature using a three-electrode, one compartment cell containing 125 ml of  $\text{H}_2\text{SO}_4$  solution at pH 1. A saturated calomel electrode (SCE) was used as reference electrode. Before starting the RRDE experiments, the appropriate gas (pure  $\text{O}_2$  or pure nitrogen) was bubbled through the electrolyte for more than 20 min and kept bubbling at a reduced rate during measurements. An activation of the platinum ring was performed just before each experiment, i.e. the ring was cycled between 1.2 and  $-0.3\text{ V}$  vs. SCE during 5 min at a scan rate of  $50\text{ mV s}^{-1}$ . Then, the potential of the disk was swept between 0.8 and  $-0.3\text{ V}$  vs. SCE at a scan rate of  $2\text{ mV s}^{-1}$ . At the same time, the ring was held at a potential fixed at  $+1.1\text{ V}$  vs. SCE in order to be in a potential region where hydrogen peroxide released by the disk is oxidized and this oxidation is limited by the

$\text{H}_2\text{O}_2$  diffusion to the ring. The ORR current  $I_D$  was deduced from the total disk current recorded under  $\text{O}_2$  by subtraction of the capacitive current recorded at the same potential under  $\text{N}_2$ . The ring current ( $I_R$ ) was thus used to monitor  $\text{H}_2\text{O}_2$  production.

### 2.2.2. Gas diffusion electrode

These were prepared using a commercial uncatalyzed ELAT carbon cloth from E-TEK Inc. This support consists on a plain weave carbon cloth (0.36 mm thick) wet-proofed by means of a hydrophobic fluorocarbon/carbon layer on the gas side. Samples having a diameter of 1 cm were punched into the carbon cloth and two layers of the catalyst suspension were dispersed on the electrolyte side. Each layer was made up of 10  $\mu\text{l}$  of the catalyst suspension dispersed over the surface of the carbon cloth using a micropipette. The first catalyst suspension layer was dried at room temperature for a few minutes before applying the second one. Depending on the cobalt loading of the powder catalyst in the suspension, the cobalt content onto the GDE was comprised between 0.45  $\mu\text{g cm}^{-2}$  (for 0.1 wt. % Co powder catalyst) and 9  $\mu\text{g cm}^{-2}$  (for 2 wt. % Co powder catalyst).

The experimental set-up described in Figure 1 was supplied by the research center of Electricité de France (EDF). The electrode was fed with various oxygen/nitrogen mixtures at a flow rate of 1.8 l  $\text{h}^{-1}$  under atmospheric pressure. The electrode surface area in contact with the electrolyte was about 12.6  $\text{mm}^2$  (4 mm of diameter). A three-electrode two-compartment cell containing 20 ml of  $\text{H}_2\text{SO}_4$  solution at pH 1 was used. A saturated calomel electrode was used as reference and the counter electrode was a platinum wire separated from electrolyte by a Nafion membrane.

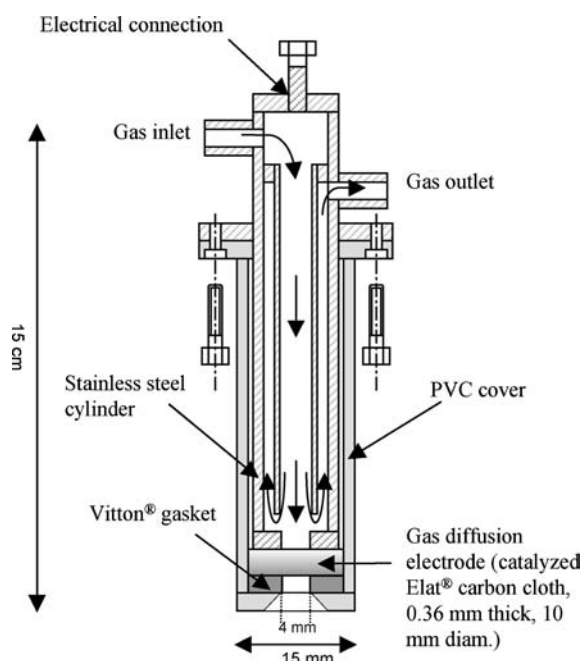


Fig. 1. Gas diffusion electrode set-up.

Electrochemical experiments were carried out using an Arbin electrochemistry testing system (model BT2043). Polarization curves were recorded at 2  $\text{mV s}^{-1}$  from 0.8 to  $-0.3$  V vs. SCE and  $\text{H}_2\text{O}_2$  electrosynthesis experiments were done for 1 h constant current ( $-1$  mA) or at constant potential ( $-150$  mV vs. SCE). The  $\text{H}_2\text{O}_2$  concentration in the electrolyte solution was determined by standard titration with  $5 \times 10^{-3}$  M  $\text{KMnO}_4$ .

## 3. Results

### 3.1. RRDE experiments

Oxygen reduction currents read for the various cobalt loadings, ranging from 0.1 to 2 wt. % Co, are reported in Figure 2a. Disk currents measured for heat-treated Vulcan without any cobalt loading are given for comparison (bold line).

It is clear in Figure 2a that the electrocatalytic activity for oxygen reduction is significantly enhanced as the cobalt loading increases. Indeed,  $I_D$  curves are shifted toward more positive potentials and the maximum currents increase. The strong positive effect of CoTMPP loading on electrode activity for ORR is mainly observed at low cobalt concentrations. No major difference for ORR activity is observed between 1 and 2 wt. % Co samples. It should be noticed that polarization curves in Figure 2a do not show any well-defined diffusion limiting current plateau but only a change in the slope of  $I_D$  vs.  $E$  curves. This behavior has already been observed for carbon supported transition metal catalysts [33, 34] and may be related to mass transport limitation in the porous structure of the catalytic coating causing a  $\text{O}_2$  concentration gradient across the coating [34]. The results presented in Figure 2a agree with other works made on pyrolyzed carbon-CoTMPP mixtures [35].

Ring currents related to the oxidation of the hydrogen peroxide produced at the disk are represented in Figure 2b. As noticed previously for the ORR, the influence of the cobalt loading is mainly observed for low cobalt concentrations. Ring currents are shifted toward more positive potentials and strongly increase as the cobalt loading increases to 0.2 wt. %. For higher Co contents, the amount of hydrogen peroxide decreases. The highest amount of hydrogen peroxide was measured for 0.2 wt. % of cobalt at a disk potential around 0.2 V vs. SCE.

Another feature that could also be noted in Figure 2b is the steady decrease in the amount of detected  $\text{H}_2\text{O}_2$  in the potential region related to mass transport limitation. The disk currents do not decrease in that potential range suggesting that  $\text{O}_2$  reduction to  $\text{H}_2\text{O}$  becomes more favorable when ORR begins to be controlled by the diffusion. This behavior is observed for all samples independently of their Co loading.

From  $I_D$  and  $I_R$  currents, it is possible to estimate the percentage of hydrogen peroxide released during the ORR (noted %  $\text{H}_2\text{O}_2$ ) by the well-known equation:

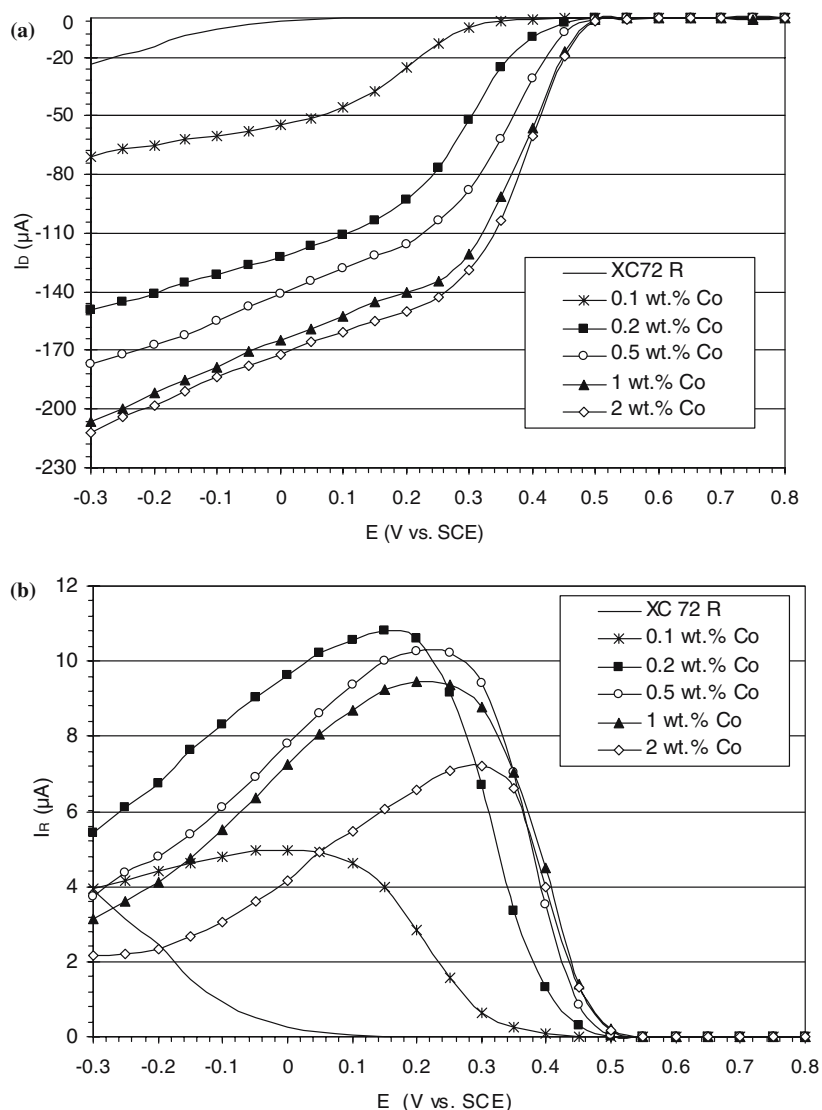


Fig. 2. Disk (a) and ring (b) currents vs. disk potential obtained from RRDE experiments for various Co loadings.

$$\%H_2O_2 = 100 \frac{2I_R/N}{|I_D| + I_R/N}$$

The values of  $\%H_2O_2$  (which also represents the selectivity of the catalyst for oxygen reduction into hydrogen peroxide) calculated for each sample are reported in Figure 3. Maximum  $\%H_2O_2$  are obtained in the potential region around 0.3–0.4 V vs. SCE. For lower potentials, a significant decrease of the  $\%H_2O_2$  is observed as the applied potential decreases. The best values of  $\%H_2O_2$  are obtained for 0.1 and 0.2 wt.% Co, reaching a maximum of 80%  $H_2O_2$  between 0.3 and 0.4 V vs. SCE. The selectivity of the catalysts decreases for higher cobalt loadings. For comparison, Vulcan alone is characterized by a value of  $\%H_2O_2$  close to 90%, occurring however at much more negative potentials (less than 0.0 V vs. SCE compared to 0.3–0.4 V for 0.2 wt.% Co). In addition, the ORR currents measured on Vulcan alone (Figure 2a) are very low compared to those measured on 0.2 wt.% Co on Vulcan, resulting in much lower  $H_2O_2$  yield.

### 3.2. GDE experiments

Oxygen reduction currents read when sweeping potential from 0.8 to  $-0.3$  V vs. SCE at  $2 \text{ mV s}^{-1}$  are presented in Figure 4. Reduction currents related to ORR continuously increase when applied potential decreases. Neither a plateau nor a change in slope appears on the GDE polarization curves, indicating that ORR is not limited by oxygen diffusion through the GDE, contrary to what seems to occur in RRDE experiments in a similar potential range.

Similarly to what was observed in Figure 2a for the RRDE measurements, the ORR also improves on GDE as the Co content increases. However, this increase in catalytic effect is only strong at low Co content and fades out as cobalt loading approaches 2 wt.% Co. Hydrogen peroxide electrosynthesis was performed at  $-1 \text{ mA}$  ( $-7.94 \text{ mA cm}^{-2}$ ) for 1 h and the Faradaic yield of hydrogen peroxide was determined by titrating with  $KMnO_4$  the amount of  $H_2O_2$  produced against the quantity of charges supplied to the GDE (two electrons

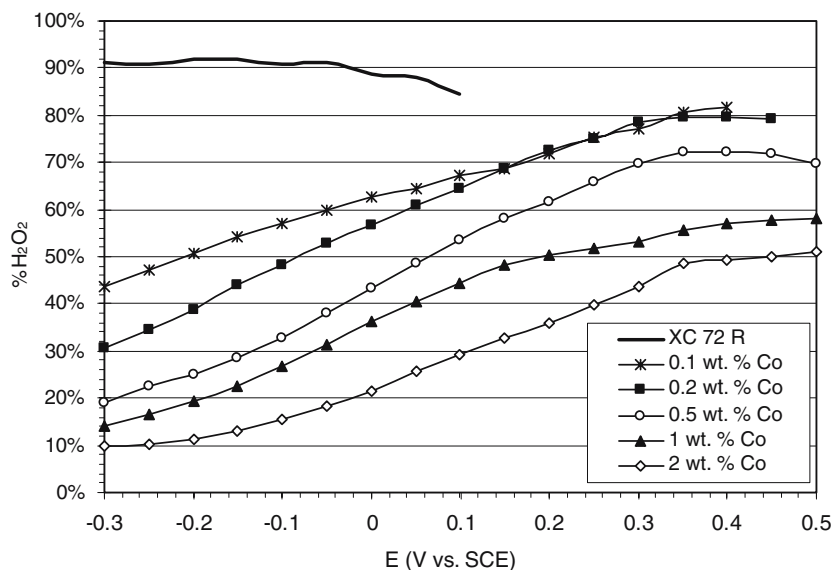


Fig. 3. Selectivity of the catalysts (expressed in %H<sub>2</sub>O<sub>2</sub>) vs. applied potential obtained from RRDE experiments for various Co loadings.

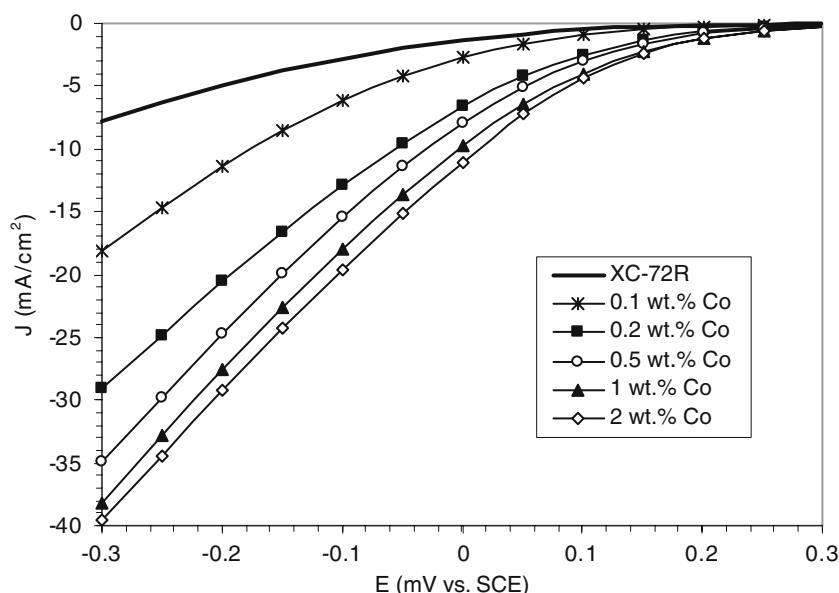


Fig. 4. Polarization curves for ORR on GDE with various Co loadings.

are necessary to produce one H<sub>2</sub>O<sub>2</sub> molecule). Steady state potential and Faradaic yields for H<sub>2</sub>O<sub>2</sub> production obtained for each sample are reported in Table 1. The highest hydrogen peroxide yield (95%) was obtained for the sample loaded at 0.2 wt. % Co. Increasing cobalt loading shifts the potential toward more positive values but reduces the hydrogen peroxide yield. Vulcan XC 72-R alone shows an H<sub>2</sub>O<sub>2</sub> yield of 75% obtained at a steady state potential as low as -434 mV vs. SCE, i.e. a potential much more negative than those measured with Co-based electrocatalysts (e.g. -17 mV for 0.2 wt. % Co). This confirms the very positive influence of pyrolyzed CoTMPP loaded on Vulcan on the GDE performance.

GDE experiments performed on heat-treated Vulcan alone at various potentials for 1 h indicate a decrease in the hydrogen peroxide yield as potential decreases

(Figure 5a, dotted line). The same behavior is observed for Co-based electrocatalysts but the decay of the H<sub>2</sub>O<sub>2</sub> yield with decreasing potential appears less marked. An example is reported for the 0.2 wt. % Co sample (Figure 5b, dotted line). One must note that the GDE performance for H<sub>2</sub>O<sub>2</sub> production is less sensitive to the applied potential in comparison to that previously observed for the same catalyst in RRDE configuration (Figure 3, dark squares).

As the production of hydrogen peroxide is potential-dependent, GDE experiments for the various samples were performed at fixed potential, i.e. -150 mV vs. SCE for 1 h. The results are reported in Table 2. The best H<sub>2</sub>O<sub>2</sub> yields were obtained on Vulcan alone as well as with 0.1 and 0.2 wt. % Co catalysts displaying a H<sub>2</sub>O<sub>2</sub> Faradaic yield higher than 90%. However, the oxygen

Table 1. Steady state potential and H<sub>2</sub>O<sub>2</sub> Faradaic yield (%H<sub>2</sub>O<sub>2</sub> titrated against current that was supplied to the GDE) obtained at 1 mA (−7.94 mA cm<sup>−2</sup>) for 1 h on GDE electrode for various cobalt loadings

	Vulcan XC 72-R	0.1 wt. % Co	0.2 wt. % Co	0.5 wt. % Co	1 wt. % Co	2 wt. % Co
<i>E</i> (mV vs. SCE)	−434	−120	−17	0	30	50
H <sub>2</sub> O <sub>2</sub> Faradaic yield (%)	75	88	95	85	78	72

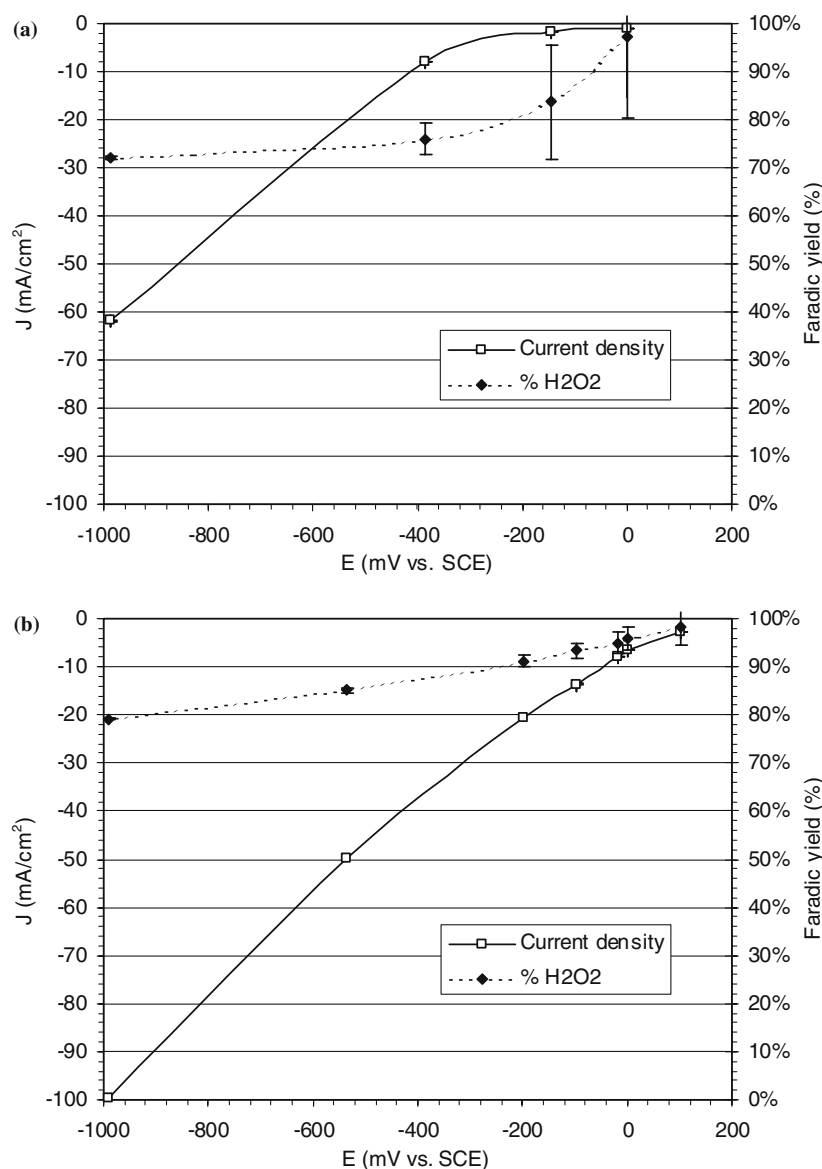


Fig. 5. Oxygen reduction current density and Faradaic yield of H<sub>2</sub>O<sub>2</sub> vs. applied potential obtained from GDE experiments with (a) Vulcan only and (b) Vulcan loaded with 0.2 wt. % Co.

reduction current density measured for a sample loaded at 0.2 wt. % Co is more than twice as large as the current density obtained on a sample loaded at 0.1 wt. % Co.

Figure 6 presents the hydrogen peroxide and water production rate after 1 h electrosynthesis at −150 mV vs. SCE using GDE with various Co loadings. Considering the electrode selectivity for the H<sub>2</sub>O<sub>2</sub> formation as well as its Faradaic yield for ORR, the best performance expressed as H<sub>2</sub>O<sub>2</sub> production rate is obtained with electrocatalysts loaded at 0.2–2 wt. % Co. The H<sub>2</sub>O<sub>2</sub> production rate reaches 300 μmol h<sup>−1</sup> cm<sup>−2</sup> compared

to 60 μmol h<sup>−1</sup> cm<sup>−2</sup> for Vulcan alone. However, as water production rate increases with the cobalt loading, it may be concluded that the best electrode for H<sub>2</sub>O<sub>2</sub> production is obtained with the electrocatalyst loaded at 0.2 wt. % Co on Vulcan.

#### 4. Discussion and conclusion

Experiments performed on RRDE and GDE indicate that the amount of hydrogen peroxide produced during

Table 2. Steady state current and H<sub>2</sub>O<sub>2</sub> Faradaic yield obtained at -150 mV vs. SCE for 1 h on GDE electrode for various cobalt loadings

	Vulcan XC 72-R	0.1 wt. % Co	0.2 wt. % Co	0.5 wt. % Co	1 wt. % Co	2 wt. % Co
$J$ (mA cm <sup>-2</sup> )	-4.2	-6.7	-17.7	-19.8	-22.4	-23.4
H <sub>2</sub> O <sub>2</sub> Faradaic yield (%)	92	96	92	81	73	67

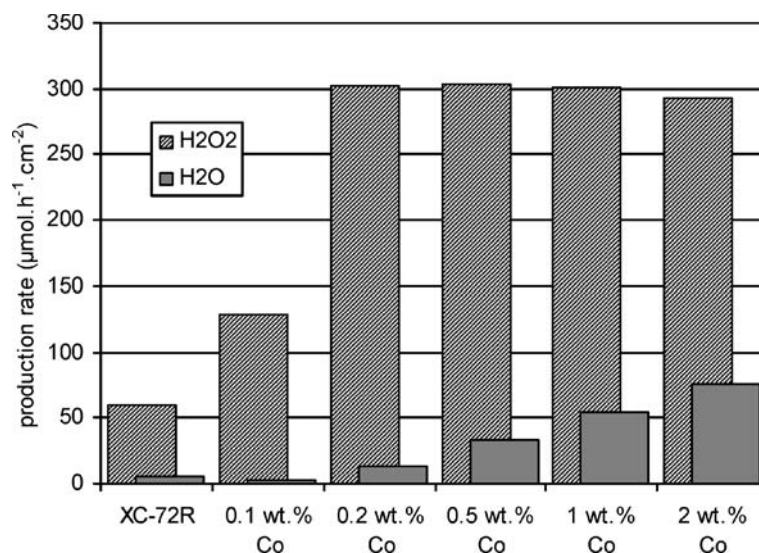
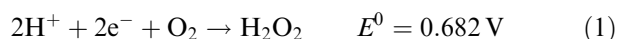
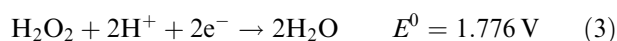


Fig. 6. Hydrogen peroxide and water production rate per hour for an electrocatalysis at -150 mV/SCE using GDE with various cobalt loadings.

ORR depends both on cobalt loading and applied potential. To interpret these results we need to express the possible electrochemical reactions occurring during ORR. In acidic solutions, oxygen reduction proceeds via two different pathways:



Reaction (1) may be followed by a reaction leading to the reduction of hydrogen peroxide into water:



On Vulcan alone, the percentage of hydrogen peroxide produced during ORR is rather high: close to 90% at potentials more positive than -300 mV/SCE (see % H<sub>2</sub>O<sub>2</sub> in Figure 3 and Faradaic yield in Figure 5a). This behavior means that, on Vulcan alone, oxygen is mainly reduced via the two-electron process of the reaction (1). However, despite their high selectivity for the two-electron oxygen reduction, H<sub>2</sub>O<sub>2</sub> production rate of Vulcan alone is very poor (Figure 6) due to the low current developed during ORR even at very low potentials (Figures 2a and 4). This illustrates the poor activity or the very limited number of catalytic sites for ORR on unmodified Vulcan.

For low cobalt loading ( $\leq 0.2$  wt. % Co), the ORR current increases drastically with cobalt loading (see Figures 2a and 4). It confirms the very positive effect of Co-based electrocatalytic sites on ORR. The percentage of produced hydrogen peroxide reaches a maximum of 80% on RRDE and more than 90% on GDE (see %H<sub>2</sub>O<sub>2</sub> in Figure 3 and Faradaic yield in Figure 5b, respectively). According to this high activity for H<sub>2</sub>O<sub>2</sub> production, we can conclude that oxygen is mainly reduced to hydrogen peroxide by catalytic sites formed on Vulcan during the heat treatment of the CoTMPP/Vulcan material.

When cobalt loading is larger than 0.2 wt. %, oxygen reduction current still increases (see Figures 2a and 4) while the amount of produced hydrogen peroxide either decreases (Figure 3) or remains constant (Figure 6). In both cases, Co loadings larger than 0.2 wt. % result in a decrease of the selectivity of the catalysts for H<sub>2</sub>O<sub>2</sub> formation. A possible explanation for that behavior is that a fraction of the H<sub>2</sub>O<sub>2</sub> produced on one Co-based catalytic site may be reduced on another catalytic site before leaving the catalytic layer. The event of those consecutive 2e<sup>-</sup> reactions will be favored by an increase of the catalytic site density and therefore, by an increase of the cobalt loading. Independently of the Co loading, the fraction of H<sub>2</sub>O<sub>2</sub> that is further reduced to water (reaction 3) becomes larger as the applied potential decreases and electron transfer is facilitated (see Figures 3 and 5).

In addition, current increases continuously as the potential decreases on GDE (Figure 4) in contrast to

RRDE experiment where the  $I_D$  slope decreases drastically from potential lower than 0.2–0.3 V (Figure 2a). It may reflect the rapid  $O_2$  diffusion through the GDE and then, ORR occurs in the mixed control zone (ORR is controlled by both electron and mass transfers), i.e. the diffusion control zone is not reached in the studied potential range. In RRDE tests, oxygen must diffuse in the electrolyte solution before to reach the catalytic layer. This process is expected to be slow in comparison to  $O_2$  diffusion in the GDE and becomes rapidly the limiting step as the potential decreases.

To conclude, the electrochemical performance of the GDE modified with pyrolyzed CoTMPP (0.2 wt. % Co)/Vulcan for the production of  $H_2O_2$  is very promising in terms of energy efficiency [36] due to its high selectivity and low overpotential for the two-electron reduction of oxygen. Moreover, its cost appears very competitive (<5 US \$ per g of catalyst) due to the low amount of CoTMPP required to obtain the maximum of electroactivity. However, the long-term stability of this electrocatalyst has to be confirmed (test in progress) before considering its use for the production of  $H_2O_2$  at the industrial scale.

### Acknowledgements

This work was supported by Electricité de France (EDF).

### References

1. W.T. Hess, 'Hydrogen peroxide' Kirk-Othmer Encyclopedia of Chemical Technology, vol. 13, 4th ed. (John Wiley & Sons, New York), p. 961.
2. H.J. Riedl and G. Pfeleiderer, US Patent 2,158,525 (1939).
3. C. Oloman and A.P. Watkinson, *J. Appl. Electrochem.* **9** (1979) 117.
4. N. Yamada, T. Yaguchi, H. Otsuka and M. Sudoh, *J. Electrochem. Soc.* **146** (1999) 2587.
5. C.W. Oloman and A.P. Watkinson, US Patent 3,969,201 (1976).
6. G.V. Kornienko, T.A. Kenova, Y.V. Saltykov, N.V. Chaenko and V.L. Kornienko, *Russ. J. Electrochem.* **34** (1998) 561.
7. Y.V. Saltykov, G.V. Kornienko, T.A. Kenova and V.L. Kornienko, *Russ. J. Electrochem.* **36** (2000) 1314.
8. E. Brillas, F. Alcaide and P.-L. Cabot, *Electrochim. Acta* **48** (2002) 331.
9. I. Yamanaka, T. Onizawa, S. Takenaka and K. Otsuka, *Angew. Chem., Int. Ed.* **42** (2003) 3653.
10. M.S. Saha, A. Denggerile, Y. Nishiki, T. Furuta and T. Ohsaka, *Electrochem. Comm.* **5** (2003) 445.
11. M. Maja, P. Tosco, and M. Vanni, *J. Electrochem. Soc.* **148** (2001).
12. K. Sundmacher and U. Hoffmann, *J. Appl. Electrochem.* **28** (1998) 359.
13. K. Wiesener, *Electrochim. Acta* **31** (1986) 1073.
14. A.L. Bouwkamp-Wijnoltz, W. Visscher, J.A.R. van Veen and S.C. Tang, *Electrochim. Acta* **45** (1999) 379.
15. J.A.R. van Veen, J.F. van Baar and J.K. Kroese, *J. Chem., Soc., Farad. Trans. 1* **77** (1981) 2827.
16. J.A.R. van Veen, H.A. Colijn and J.F. van Baar, *Electrochim. Acta* **33** (1988) 801.
17. C. Mocchi and S. Trasatti, *J. Mol. Catal. A: Chem.* **204–205** (2003) 713.
18. P. He, M. Lefèvre, G. Faubert and J.P. Dodelet, *J. New Mater. Electrochem. Syst.* **2** (1999) 243.
19. G. Lalande, R. Côté, D. Guay, J.P. Dodelet, L.T. Weng and P. Bertrand, *Electrochim. Acta* **42** (1997) 1379.
20. S. Gupta, D. Tryk, I. Brae, W. Alred and E. Yeager, *J. Appl. Electrochem.* **19** (1989) 19.
21. G. Faubert, R. Côté, D. Guay, J.P. Dodelet, G. Dénès, C. Poleunis and P. Bertrand, *Electrochim. Acta* **43** (1998) 1969.
22. T. Okada, S. Gotou, M. Yoshida, M. Yuasa, T. Hirose and I. Sekine, *J. Inorg. Organometal. Polymers* **9** (1999) 199.
23. G. Wei, J.S. Wainright and F.R. Savinell, *J. New Mater. Electrochem. Syst.* **3** (2000) 121.
24. M. Bron, J. Radnik, M. Fieber-Erdmann, P. Bogdanoff and S. Fiechter, *J. Electroanal. Chem.* **535** (2002) 113.
25. S. Marcotte, D. Villers, N. Guillet, L. Roué and J.P. Dodelet, *Electrochim. Acta* **50** (2004) 179.
26. E. Claude, T. Addou, M.J. Latour and P. Aldebert, *J. Appl. Electrochem.* **28** (1998) 57.
27. F. Jaouen, S. Marcotte, J.P. Dodelet and G. Lindbergh, *J. Phys. Chem. B* **107** (2003) 1376.
28. J. Zagal, P. Bindra and E. Yeager, *J. Electrochem. Soc.* **127** (1980) 1506.
29. R. Jiang and D. Chu, *J. Electrochem. Soc.* **147** (2000) 4605.
30. M. Lefèvre and J.P. Dodelet, *Electrochim. Acta* **48** (2003) 2749.
31. J. Maruyama, M. Inaba, T. Morita and Z. Ogumi, *J. Electroanal. Chem.* **504** (2001) 208.
32. Z. Ogumi, T. Kuroe and Z.-i. Takehara, *J. Electrochem. Soc.* **132** (1985) 2601.
33. A.L. Bouwkamp-Wijnoltz, W. Visscher and J.A.R. van Veen, *Electrochim. Acta* **43** (1998) 3141.
34. S. Ye and A. K. Vijn, *Electrochem. Comm.* **5** (2003) 272.
35. V.S. Tyurin, K.A. Radyushkina, O.A. Levina and M.R. Tarasevich, *Russ. J. Electrochem.* **37** (2001) 843.
36. N. Chhim S. Trévin, N. Aliouane, S. Marcotte, N. Guillet, L. Roué, and J.P. Dodelet, pending patent FR 040261 (2004).